European Journal of Medicinal Chemistry 76 (2014) 1–9

Contents lists available at ScienceDirect

European Journal of Medicinal Chemistry

journal homepage: http://www.elsevier.com/locate/ejmech

Original article

Identification of a new series of amides as non-covalent proteasome inhibitors

Kety Scarbaci [a], Valeria Troiano [a], Nicola Micale [a], Roberta Ettari [b,*], Lucia Tamborini [b], Carmen Di Giovanni [c], Carmen Cerchia [c], Silvana Grasso [a], Ettore Novellino [c], Tanja Schirmeister [d], Antonio Lavecchia [c], Maria Zappalà [a]

[a] Dipartimento di Scienze del Farmaco e dei Prodotti per la Salute, Università degli Studi di Messina, Viale Annunziata, 98168 Messina, Italy
[b] Dipartimento di Scienze Farmaceutiche, Università degli Studi di Milano, Via Mangiagalli 25, 20133 Milano, Italy
[c] Dipartimento di Farmacia, "Drug Discovery" Laboratory, Università degli Studi di Napoli Federico II, Via Domenico Montesano 49, 80131 Napoli, Italy
[d] Institute of Pharmacy and Biochemistry, University of Mainz, Staudinger Weg 5, D-55099 Mainz, Germany

ARTICLE INFO

Article history:
Received 17 July 2013
Received in revised form
14 January 2014
Accepted 16 January 2014
Available online 25 January 2014

Keywords:
Amides
Proteasome inhibitors
Non-covalent inhibitors
Docking studies

ABSTRACT

Proteasome inhibition has emerged as an important therapeutic strategy for the treatment of multiple myeloma (MM) and some forms of lymphoma, with potential application in other types of cancers. 20S proteasome consists of three different catalytic activities known as chymotrypsin-like (ChT-L), trypsin-like (T-L), and, post-glutamyl peptide hydrolyzing (PGPH) or caspase-like (C-L), which are located respectively on the β5, β2, and β1 subunits of each heptameric β rings. Currently a wide number of covalent proteasome inhibitors are reported in literature; however, the less widely investigated non-covalent inhibitors might be a promising alternative to employ in therapy, because of the lack of all drawbacks and side-effects related to irreversible inhibition. In the present work we identified a series of amides, two of which (**1b** and **1f**) are good candidates to non-covalent inhibition of the chymotrypsin-like activity of the β5 proteasome subunit. The non-covalent binding mode was corroborated by docking simulations of the most active inhibitors **1b**, **1f** and **2h** into the yeast 20S proteasome crystal structure.

1. Introduction

The eukaryotic 26S proteasome is a large (1.6–2.4 MDa) multi-functional particle, composed of a barrel-shaped 20S catalytic core capped by two 19S regulatory complexes. The 20S proteasome is the proteolytically active key element of the ubiquitin–proteasome system. It is composed by four heptameric rings stacked in a $\alpha_7\beta_7\beta_7\alpha_7$ arrangement and contains three proteolytic subunits, β1, β2 and β5, which have distinct substrate specificities and are responsible, respectively, for the caspase-, trypsin- and chymotrypsin-like activities of proteasome [1]. All the three subunits possess a catalytic site that employs the nucleophilic γ-hydroxyl group of the N-terminal Thr to cleave peptide bonds [2]. The expression of these subunits in normal cells may be replaced by the synthesis of the immunoproteasome catalytic subunits counterparts β1i, β2i and β5i (>50% of identity; also named LMP2, MECL1 and LMP7, respectively) upon exposure to specific stimuli such as the inflammatory cytokines IFN-γ and TNF-α [3].

Proteasome is responsible for the turnover of cellular proteins that regulate cell proliferation and survival pathways, however defects of its proteolytic activity can lead to anarchic cell proliferation and as a consequence to tumor development.

It has been demonstrated that inhibition of the chymotrypsin-like (ChT-L) activity of proteasome represents a valid strategy to induce antineoplastic effects in hematologic tumors [4]. A growing number of studies suggest that proteasome inhibitors may become valuable drugs for the treatment of nontumorous diseases when used in conditions in which the cellular functions are modulated without induction of cell death [5]. Diverse beneficial effects are expected in inflammation [6], neurodegenerative diseases [7], muscular dystrophies [8] and cachexia [9]. Moreover, they have therapeutic potential as antiparasitics in malaria [10] and sleeping syndrome [11] and as antimicrobial agents (tuberculosis) [12].

The majority of 20S proteasome inhibitors, currently reported in literature [13], are peptide-based compounds, endowed with a C-terminal electrophilic warhead that forms covalent adducts with the active site Thr1Oγ (Fig. 1a, for bortezomib). A reversible action

Abbreviations: ChT-L, chymotrypsin-like; T-L, trypsin-like; PGPH, post-glutamyl peptide hydrolyzing; C-L, caspase-like; DMSO, dimethyl sulfoxide; EDC, 1-ethyl-3-(3-dimethylaminopropyl)carbodiimide; HOBt, *N*-hydroxybenzotriazole; DIPEA, *N*,*N*-diisopropylethylamine.

* Corresponding author. Tel.: +39 02 50319342; fax: +39 02 50319359.
E-mail address: roberta.ettari@unimi.it (R. Ettari).

0223-5234/$ – see front matter © 2014 Elsevier Masson SAS. All rights reserved.
http://dx.doi.org/10.1016/j.ejmech.2014.01.022

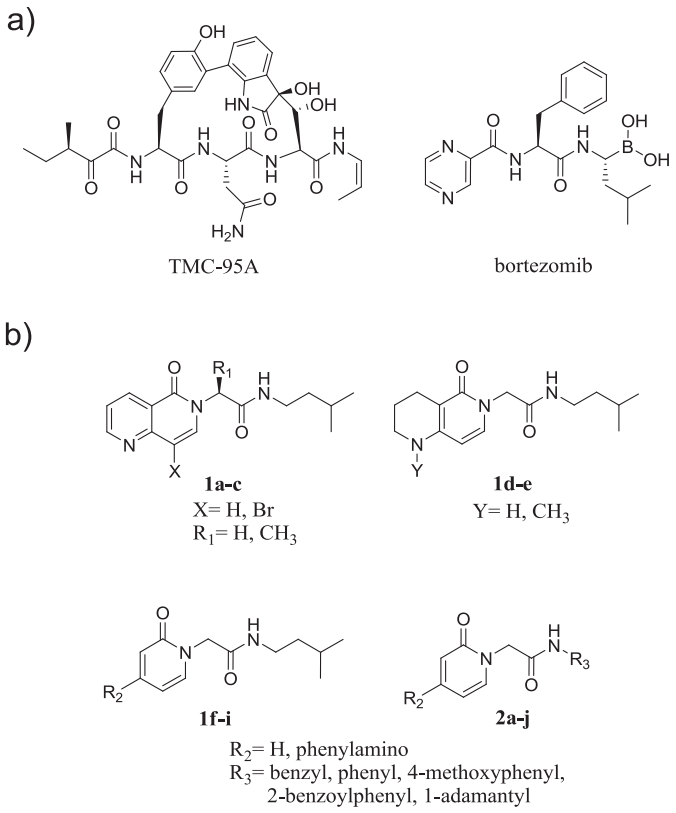

Fig. 1. Structure of representative non-covalent (TMC-95A), covalent (bortezomib) proteasome inhibitors (a) and amides **1**–**2** (b).

characterizes aldehydes, α-keto-aldehydes, α-keto-oxadiazoles, β-lactones, boronates. α′,β′-Epoxyketones are characterized by an irreversible action. Very often this covalent mode of action, together with high reactivity of compounds, may lead to off-target interactions.

In this context, the dipeptide boronate Bortezomib (Velcade®), the first proteasome inhibitor approved by the FDA for treatment of multiple myeloma and mantle cell lymphoma, has been demonstrated to possess low systemic tissue distribution, severe off-target effects due to lack of specificity [14]. Despite the dipeptide boronates reversibly interact with the target enzyme, the formation of a long-lasting inhibitor-proteasome adduct is responsible of its unfavorable pharmacodynamic profile: when it is injected intravenously a big part of administered dose inhibits the chymotrypsin-like activity of 20S proteasome of non-tumor cells, like hematic or liver cells. As a consequence while irreversible blockage of an enzyme should be advantageous for parasitic targets [15], on the contrary in the case of cancer treatment, non-covalent inhibition would be desirable. Thus, there is a recent tendency to identify non-covalent inhibitors, like TMC-95A, (Fig. 1 a) and its linear derivatives [16].

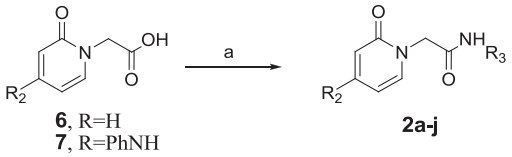

Scheme 2. Reagents and conditions: a) HOBt, EDC·HCl, then suitable amine and DIPEA, CH_2Cl_2, −0 °C → rt, 12 h.

Non-covalent inhibitors, even if less widely investigated, with respect to covalent inhibitors, provide an alternative mechanism for proteasome inhibition and, due to the rapid dissociation from the 20S subunits, may be devoid of all drawbacks related to either irreversible or slowly reversible enzyme inhibition. Their potential advantages are improved selectivity, moderate reactivity and reduced instability, which are often associated with side effects in therapeutics [17]. Taking into account all these reasons non-covalent proteasome inhibitors might be a promising alternative for therapy.

Our research group has been involved in the last years in the development of peptidomimetic vinyl sulfones [18] and boronates [19] as irreversible and pseudo-irreversible 20S proteasome inhibitors, respectively. During the development of peptidomimetic boronates, we identified a number of amides **1** (Fig. 1 b), recovered as by-products of the key step for the introduction of the boronic ester moiety. After a preliminary screening, some of these molecules were supposed to non-covalently inhibit β5 proteasome subunit. Starting from these findings, and on the basis of a docking model, we synthesized and evaluated as potential 20S proteasome inhibitors a second series of amides **2** (Fig. 1 b), in which bulkier substituents directly linked to the amide moiety, in agreement also to literature data [20], have been introduced in order to extend the structure–activity relationship of this class of molecules.

2. Results and discussion

2.1. Chemistry

In our multistep approach for the synthesis of peptidomimetic boronates, carried out with our previously reported procedure [19], we identified compounds **1** as by-products. More in detail the synthetic step leading to the introduction of the pharmacophore portion, realized by coupling the carboxylic acids **3** and pinanediol leucine boronate **4** in the presence of EDC·HCl, HOBt and DIPEA, together with the desired product **5**, led to the formation, as minor reaction product, of amides **1** obtained by spontaneous deboronation of boronic esters **5** (Scheme 1).

The synthesis of amides **2a**–**c**, **2e**–**h** and **2j** (Scheme 2) has been carried out by coupling acid **6** or **7**, synthesized according to a previously reported procedure [19], together with the suitable amines by employing also in this case, HOBt and EDC·HCl as coupling reagents to get the desired amides in high yields. Different conditions were adopted for the synthesis of sterically hindered amides **2d** and **2i**, in this case acid **6** or **7** was first activated to mixed

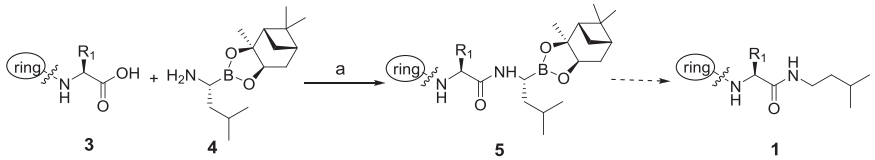

ring = 1*H*-pyridin-2-one or 1,6-naphthyridin-5(6*H*)-one

Scheme 1. Reagents and conditions: (a) HOBt, CH_2Cl_2, −5 °C, 20 min, then EDC·HCl, DIPEA, **7**, −15 °C → rt, 3 h.

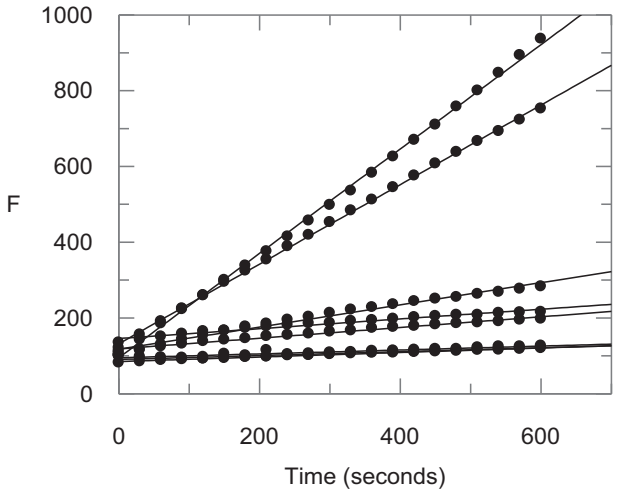

Fig. 2. Progress curve of substrate hydrolysis in presence of the inhibitors **1f**. F = fluorescence units. Inhibitor concentrations (from top to bottom): 0, 1.0, 10.0, 20.0, 40.0, 60.0, 80.0, 100.0 μM.

anhydride, by employing *N*-methylmorpholine and isobutylchloroformate, and then coupled with 2-aminobenzophenone.

2.2. Biological activity and docking studies

Early reports attest the great stability of alkylboronic acids under aqueous acidic solutions, as a matter of fact simple alkylboronic acids can be heated in 40% aqueous HBr or HI [21], without any decomposition. However, deboronation has been quite often observed in basic aqueous solutions [22], thus allowing us to explain the formation from the boronic ester of the corresponding amide, probably because of the addition of DIPEA, during the coupling reaction.

With the aim to evaluate their inhibitory properties, we screened amides **1a**–**i** at 20 μM against the three 20S proteasome proteolytic activities (ChT-L, T-L, PGPH), in such a way to evaluate their potential ability to inhibit the target enzyme. For compounds which passed the initial screening (at least 40% of inhibition), additional assays were performed. The dissociation constants K_i of the non covalent complex E·I were obtained from the progress curves at seven different concentrations of inhibitor, as reported in Fig. 2 for inhibitor **1f**, by fitting the progress curves to the 4-parameter IC_{50} equation:

$$y = \frac{y_{max} - y_{min}}{1 + \left(\frac{[I]}{IC_{50}}\right)^{s}} + y_{min}$$

(with y[dF/min] as the substrate hydrolysis rate, y_{max} as the maximum value of the dose–response curve that is observed at very low inhibitor concentrations, y_{min} as the minimum value that is obtained at high inhibitor concentrations, and s denotes the Hill coefficient, and correction to zero substrate concentration from $K_i = IC_{50}/(1 + [S]\,K_m^{-1})$.

In this regard compounds **1b** and **1f** were proven to be the most active compounds, with K_i values of 0.56 and 0.33 μM, respectively (Table 1).

Table 1
Inhibition of ChT-L proteasome activity by amides **1a**–**i**.

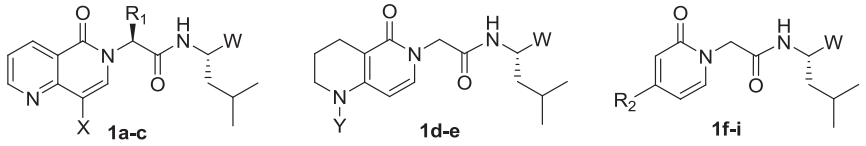

1, W = H
1-BA, W = $B(OH)_2$

Comp	X	R_1	Y	R_2	ChT-L	
					K_i (μM)[a]	% inhib. at 20 μM
1a	H	H	–	–	n.d.	10
1a-BA[c]	H	H	–	–	0.44 ± 0.21	100
1b	Br	H	–	–	0.56 ± 0.01	56
1b-BA[c]	Br	H	–	–	0.17 ± 0.01	100
1c	H	Methyl	–	–	n.d.	35
1c-BA[c]	H	Methyl	–	–	1.34 ± 0.12	100
1d	–	–	H	–	10.1 ± 0.9	45
1e	–	–	Methyl	–	n.d.	7
1e-BA[c]	–	–	Methyl	–	1.62 ± 0.44	84
1f	–	–	–	Phenylamino	0.33 ± 0.05	87
1f-BA[c]	–	–	–	Phenylamino	0.098 ± 0.005	97
1g	–	–	–	Diethylamino	n.d.	28
1g-BA[c]	–	–	–	Diethylamino	0.80 ± 0.11	100
1h	–	–	–	Morpholin-4-yl	7.67 ± 0.23	42
1h-BA[c]	–	–	–	Morpholin-4-yl	1.45 ± 0.04	100
1i	–	–	–	Piperidin-1-yl	n.d.	27
1i-BA[c]	–	–	–	Piperidin-1-yl	0.30 ± 0.05	88
Bortezomib[b]					0.0098 ± 0.001	100

n.d. = not determined.
BA = boronic acid.
[a] Values represent the mean of three independent determinations.
[b] Values determined in the same experimental conditions of compounds **1**.
[c] For comparison, corresponding boronates (**1-BA***) [19] and bortezomib are added as reference covalent compounds.

Compound **1b**, turned also to be active on the PGPH activity, with a K_i value of 22.3 μM. This outcome is extremely important taking into consideration that co-inhibition of β5 subunits with either β1 or β2 subunits exerts the maximal effect that is required to produce an antitumor response.

A comparison between the amides of the present work and the corresponding boronates (**1-BA** [19], Table 1) clearly points out the better inhibitory activity of the compounds bearing the boronic acid moiety with respect to the ones that are lacking such a warhead. However, in some cases the inhibitory activity revealed to be almost comparable (e.g. **1b** and **1b-BA** with K_i values of 0.56 and 0.17 μM respectively) and this highlights how both inhibitors are able to establish key interactions with the target enzyme, even if with a different mode of action.

Inhibitors **1b** and **1f** were docked into the binding pocket of the β5 subunit (Fig. 3), using the crystal structure of bortezomib bound to the yeast 20S proteasome (PDB ID: 2F16) [23].

Docking simulations clearly displayed **1b** and **1f** in the proximity of the ChT-L active site in subunit β5 and suggested a non-covalent mode of binding. The ligands did not interact with the active-site β5-T1 O^{γ} nucleophile, which hitherto has been considered a common principle of ChT-L inhibitor binding. The isopentyl group linked to the amide moiety of compounds **1b** and **1f** projected into the S1 pocket, adopting a spatial arrangement similar to that of the P1-leucine side chain of bortezomib. Both compounds accommodated their aromatic group perfectly in the S3 pocket through a series of van der Waals interactions, thereby profoundly stabilizing these moieties in the ChT-L site. In addition, the amide and the pyridinone C═O oxygens of both ligands are predicted to form H-bonds with β5-A49N, β5-A50N and β6-D114O^{γ} *via* an intervening water molecule located crystallographically in the bortezomib structure and included in our model. It is to note that compound **1f** engaged a further H-bond with β5-T21 NH backbone through its amide C═O group. Interestingly, both compounds are predicted to establish an H-bond with the side chain of D114 of the β6 subunit, and this could explain the higher activity of **1b** and **1f** with respect to the other tested derivatives. Specifically, the 8-bromo-naphthyridinone C═O of **1b** and the 4-phenylamino NH of **1f** established an H-bond with the protonated β6-D114, thus contributing to the stabilization of both inhibitors.

With this in mind, we developed a series of 4-amino-substituted pyridone analogs **2f**–**j**, with the aim to extend the structure–activity relationship of this class of molecules. The corresponding unsubstituted analogs **2a**–**e** were also synthesized to assess the relevance of the phenylamino moiety at position 4 of the pyridone nucleus. At P1 site, to evaluate the size of the liphophilic pocket that normally accommodates the isopentyl group, we introduced bulkier substituents, like aromatic or alicyclic nuclei (e.g. phenyl, adamantyl).

From a preliminary screening at 20 μM amides **2a**–**j** were proven to weakly inhibit the β5 subunit of 20S proteasome, with the exception of compounds **2e**, **2h** and **2i**, which showed K_i values of 7.55, 1.48 and 8.03 μM respectively (Table 2).

The amide **2h** revealed to be the most active compound of this series of analogs, in agreement with its presumed ability to form an H-bond with D114 of the β6 subunit, similarly to amide **1f**. Overall only the 4-methoxyphenyl substituent directly linked to the amide function (i.e. **2h**) yielded an activity nearly comparable to that of **1f**, bearing an isopentyl group. However, from a general analysis of the obtained results, the isopentyl substituent, in terms of size, proved to be optimal for the correct alignment of the inhibitor in the binding site. Additionally compounds **2e**, **2h** and **2i** were proven to co-inhibit the PGPH activity of the 20S proteasome (more then 50% of inhibition at 20 μM) that, as already said, is desirable to enhance an antitumor response.

Interestingly, docking of **2h** to the ChT-L active site of the yeast proteasome revealed that it, unlike compounds **1b**, **1f** and bortezomib, did not bind into the S1 region of the ChT-L pocket but in the S2 and S3 regions between the subunits β5 and β6 (Fig. 4a). In addition to forming H-bonds with β5-G47, β5-T21, β5-A49 and β6-D114, **2h** accepted a further H-bond from β5-S129 through its 4-methoxy oxygen atom, thus stabilizing the position of the 4-

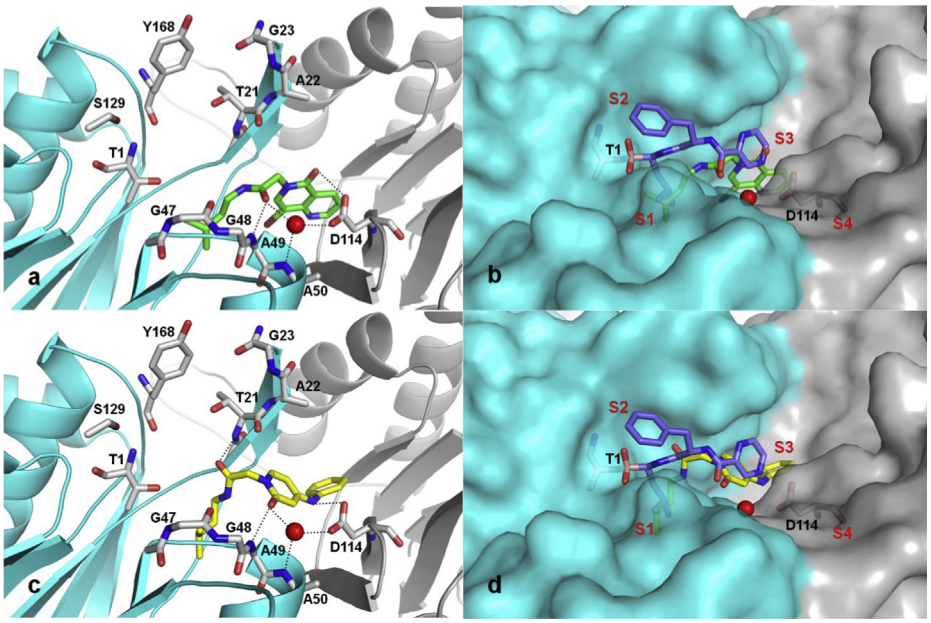

Fig. 3. Binding modes of compounds **1b** (a, green), and **1f** (c, yellow) into the β5 (cyan)/β6 (white) active site of 20S proteasome represented as a ribbon model (PDB ID: 2F16) [20]. Only amino acids located within 4 Å of the bound ligand are displayed (white) and labeled. Key H-bonds between the inhibitors and the protein are shown as dashed black lines. An overlay of **1b** (b, docked pose), **1f** (d, docked pose) with bortezomib (purple, X-ray crystal pose) is shown in the β5/β6 active site of 20S proteasome displayed as Connolly surface. The defined water molecule forming tight H-bonds to the protein is shown as a red sphere. Specificity pockets S1–S4 are indicated. (For interpretation of the references to colour in this figure legend, the reader is referred to the web version of this article.)

Table 2
Inhibition of ChT-L proteasome activity by amides **2a**–**j**.

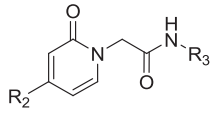

2a-j

Comp	R_2	R_3	ChT-L	
			K_i (μM)[a]	% inhib. at 20 μM
2a	H	Benzyl	n.d.	15
2b	H	Phenyl	n.d.	23
2c	H	4-Methoxyphenyl	n.d.	32
2d	H	2-Benzoylphenyl	n.d.	21
2e	H	1-Adamantyl	7.55 ± 0.86	86
2f	Phenylamino	Benzyl	n.d.	16
2g	Phenylamino	Phenyl	n.d.	9
2h	Phenylamino	4-Methoxyphenyl	1.48 ± 0.06	72
2i	Phenylamino	2-Benzoylphenyl	8.03 ± 0.25	67
2j	Phenylamino	1-Adamantyl	n.d.	13

n.d. = not determined.
[a] Values represent the mean of three independent determinations.

methoxyphenyl moiety in the S2 pocket. This explains the high affinity of **2h** to the ChT-L active site in comparison with compounds **2g** and **2f**.

Structural superposition of **1f** and **2h** (Fig. 4b) bound to the ChT-L active site clearly suggests that the decrease in affinity of compounds having a bulkier substituent in R_3 (**2f**–**j**) is due to three main residues in the S1 site (Fig. 4, Table 2), M45, V31, and A49 of subunit β5, which create a steric barrier to the P1 R_3 moiety. Similarly, engineered derivatives of omuralide [2] and salinosporamide A [24], with a phenyl moiety in P1, have been demonstrated to exert significantly reduced inhibitory potency toward the ChT-L activity of yeast proteasome compared to the natural products [25] These P1 side chain examples highlight the high degree of proteasomal substrate binding channel plasticity, which shows the complexity of optimizing the binding profile of proteasome inhibitors.

To assess the selectivity for the target enzyme, amides **1**–**2** were tested on bovine pancreatic α-chymotrypsin and cathepsin B. None of them showed no significant inhibition in the selectivity assays, with the exception of compound **2i**, which gave a K_i value of 6.65 μM against bovine pancreatic α-chymotrypsin.

To evaluate the cytotoxic and/or growth inhibitory effects, all synthesized compounds were submitted for testing at the National Cancer Institute NCI. Ten amides (**1a**, **1e**–**h**, **2d**, **2g**–**j**) were selected for a primary in vitro antitumor assay. Each compound was routinely tested, at 10^{-5} M concentration, against 60 human tumor cell lines, unfortunately within the one dose all compounds turned out to be essentially inactive.

In conclusions with our work we identified a series of amides, some of which turned to be active against the chymotrypsin-like activity of 20S proteasome. In particular compounds **1b** and **1f** were proven to possess K_i values in the submicromolar range, thus being reasonable to consider them worthy of further optimization within the development of non-covalent 20S proteasome inhibitors for cancer treatment.

3. Experimental protocols

3.1. Chemistry

All reagents and solvents were obtained from commercial suppliers and were used without further purification. Reactions under microwave irradiation were performed on a CEM Discover apparatus. Elemental analyses were carried out on a C. Erba Model 1106 (Elemental Analyzer for C, H and N) and the obtained results are within ±0.4% of the theoretical values. Merck Silica Gel 60 F_{254} plates were used as analytical TLC; flash column chromatography was performed on Merck Silica Gel (200–400 mesh). ^{1}H NMR spectra were recorded on a Varian Gemini 300 MHz spectrometer using the residual signal of the deuterated solvent as internal standard. Splitting patterns are described as singlet (s), doublet (d), doublet of doublet (dd), triplet (t), quartet (q), multiplet (m) and broad singlet (bs). ^{1}H chemical shifts are expressed in δ (ppm) and coupling constants (*J*) in hertz (Hz).

3.2. General procedure for the synthesis of compounds *1*

Compounds **1** have been obtained as by-products of the coupling reaction between the carboxylic acids **3** and pinanediol leucine boronate **4**, employed for the introduction of boronic ester moiety, as previously reported [17].

3.2.1. *N-Isopentyl-2-(5-oxo-1,6-naphthyridin-6(5H)-yl)acetamide (**1a**)*

Yield 11%. R_f = 0.38 ($CHCl_3$/MeOH 95:5). ^{1}H NMR (300 MHz, $CDCl_3$) δ 0.87 (d, 6H, *J* = 6.6 Hz), 1.37 (q, 2H, *J* = 7.5 Hz), 1.50–1.62 (m, 1H), 3.22–3.29 (m, 2H), 4.60 (s, 1H), 6.43 (bs, 1H), 6.85 (d, 1H, *J* = 7.1 Hz), 7.42 (d, 1H, *J* = 7.1 Hz), 7.43 (dd, 1H, *J* = 8.0, 4.9 Hz), 8.66 (dd, 1H, *J* = 8.0, 1.8 Hz), 8.94 (dd, 1H, 8.0, 1.8 Hz). Anal. Calcd. for $C_{15}H_{19}N_3O_2$: C 65.91, H 7.01, N 15.37. Found: C 65.73, H 7.22, N 15.42.

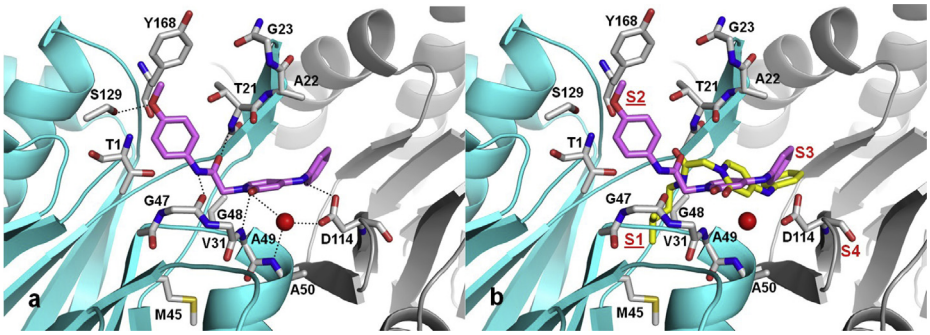

Fig. 4. a) Binding mode of compound **2h** (magenta) into the β5 (cyan)/β6 (white) active site of 20S proteasome represented as a ribbon model (PDB ID: 2F16) [20]. Only amino acids located within 4 Å of the bound ligand are displayed (white) and labeled. Key H-bonds between the inhibitor and the protein are shown as dashed black lines. b) Structural superposition of **2h** (magenta) and **1f** (yellow) is shown in the ChT-L active site of 20S proteasome. The defined water molecule forming tight H-bonds to the protein is shown as a red sphere. Specificity pockets S1–S4 are indicated. (For interpretation of the references to colour in this figure legend, the reader is referred to the web version of this article.)

*3.2.2. 2-(8-Bromo-5-oxo-1,6-naphthyridin-6(5H)-yl)-N-isopentylacetamide (**1b**)*

Yield 26%. R_f = 0.58 ($CHCl_3$/MeOH 95:5). ^1H NMR (300 MHz, $CDCl_3$) δ 0.89 (d, 6H, *J* = 5.9 Hz), 1.40 (q, 2H, *J* = 6.5 Hz), 1.50–1.64 (m, 1H), 3.28 (q, 2H, *J* = 6.5 Hz), 4.59 (s, 2H), 7.48–7.57 (m, 1H), 7.78 (s, 1H), 8.70 (d, 1H, *J* = 7.6 Hz), 9.04–9.12 (m, 1H). Anal. Calcd. for $C_{15}H_{18}BrN_3O_2$: C 51.15, H 5.15, N 11.93. Found: C 51.23, H 5.07, N 11.72.

*3.2.3. N-Isopentyl-2-(5-oxo-1,6-naphthyridin-6(5H)-yl) propanamide (**1c**)*

Yield 7%. R_f = 0.42 ($CHCl_3$/MeOH 95:5). $[\alpha]_D^{20}$ = −47.8 (*c* 0.2, $CHCl_3$); ^1H NMR (300 MHz, $CDCl_3$) δ ppm 0.85 (d, 6H, *J* = 4.69 Hz), 1.31–1.45 (m, 2H), 1.46–1.56 (m, 1H), 1.63 (d, 3H, *J* = 6.5 Hz), 3.13–3.33 (m, 2H), 5.66 (d, 1H, *J* = 6.5 Hz), 6.39 (bs, 1H), 6.86 (d, 1H, *J* = 7.0 Hz), 7.36–7.46 (m, 1H), 7.56 (d, 1H, *J* = 7.0 Hz), 8.58–8.70 (m, 1H), 8.86–8.97 (m, 1H). Anal. Calcd. for $C_{16}H_{21}N_3O_2$: C 66.88, H 7.37, N 14.62. Found: C 66.73, H 7.21, N 14.79.

*3.2.4. N-Isopentyl-2-(1,2,3,4-tetrahydro-5-oxo-1,6-naphthyridin-6(5H)-yl)acetamide (**1d**)*

Yield 13%. R_f = 0.31 ($CHCl_3$/MeOH 95:5). ^1H NMR (300 MHz, $CDCl_3$) δ ppm 0.88 (d, 6H, *J* = 6.5 Hz), 1.36 (q, 2H, *J* = 7.0 Hz), 1.50–1.64 (m, 1H), 1.85–1.96 (m, 2H), 2.58 (t, 2H, *J* = 5.9 Hz), 3.20 (q, 2H, *J* = 7.0 Hz), 3.25–3.34 (m, 2H), 4.42 (s, 2H), 5.59 (d, 1H, *J* = 7.6 Hz), 7.03 (d, 1H, *J* = 7.6 Hz). Anal. Calcd. for $C_{15}H_{23}N_3O_2$: C 64.97, H 8.36, N 15.15. Found: C 64.89, H 8.55, N 15.37.

*3.2.5. N-Isopentyl-2-(1,2,3,4-tetrahydro-1-methyl-5-oxo-1,6-naphthyridin-6(5H)-yl)acetamide (**1e**)*

Yield 40%. R_f = 0.36 ($CHCl_3$/MeOH 95:5). ^1H NMR (300 MHz, $CDCl_3$) δ 0.86 (d, 6H, *J* = 6.2 Hz), 1.32–1.39 (m, 2H), 1.46–1.62 (m, 1H), 1.86–1.96 (m, 2H), 2.56–2.60 (m, 2H), 2.95 (s, 3H), 3.15–3.26 (m, 4H), 4.43 (s, 2H), 5.86 (d, *J* = 7.6 Hz), 7.10 (d, *J* = 7.6 Hz), 7.42 (bs, 1H, NH). Anal. Calcd. for $C_{16}H_{25}N_3O_2$: C 65.95, H 8.65, N 14.42. Found: C 65.71, H 8.82, N 14.17.

*3.2.6. N-Isopentyl-2-(2-oxo-4-phenylamino-2H-pyridin-1-yl) acetamide (**1f**)*

Yield 37%. R_f = 0.43 ($CHCl_3$/MeOH 95:5). ^1H NMR (300 MHz, DMSO-d_6): δ 0.88 (d, 6H, *J* = 6.6 Hz) 1.33–1.41 (m, 3H), δ 4.53 (s, 2H), 5.90–5.93 (m, 1H), 6.15 (s, 1H), 7.09–7.72 (m, 11H), 8.55 (bs, 1H). Anal. Calcd. for $C_{18}H_{23}N_3O_2$, C 68.98, H 7.40, N 13.41. Found C 68.74, H 7.44, N 13.33.

*3.2.7. 2-(4-Diethylamino-2-oxo-2H-pyridin-1-yl)-N-isopentyl acetamide (**1g**)*

Yield 30%. R_f = 0.57 ($CHCl_3$/MeOH 95:5). ^1H NMR (300 MHz, $CDCl_3$): δ 0.88 (d, 6H, *J* = 6.6 Hz), 1.18 (t, 6H, *J* = 7.1 Hz), 1.33–1.41 (m, 2H), 1.53–1.64 (m, 1H), 3.17–3.24 (m, 2H), 3.28–3.35 (q, 4H, *J* = 7.1 Hz), 4.42 (s, 2H), 5.57 (d, 1H, *J* = 1.8 Hz), 5.85 (dd, 1H, *J* = 7.5, 1.8 Hz), 7.16 (dd, 1H, *J* = 1.3, 7.5 Hz), 7.39 (bs, 1H). Anal. Calcd. for $C_{16}H_{27}N_3O_2$, C 65.50, H 9.28, N 14.32. Found C 65.66, H 9.13, N 14.43.

*3.2.8. 2-(4-Morpholin-4-yl-2-oxo-2H-pyridin-1-yl)-N-isopentyl acetamide (**1h**)*

Yield 33%. R_f = 0.49 ($CHCl_3$/MeOH 95:5). ^1H NMR (300 MHz, $CDCl_3$): δ 0.87 (d, 6H, *J* = 5.7 Hz), 1.32–1.39 (m, 2H), 1.52–1.61 (m, 1H), 3.16–3.26 (m, 6H), 3.78 (s, 4H), 4.43 (s, 2H), 5.73 (s, 1H), 5.97 (d, 1H, *J* = 7.9 Hz), 7.22 (d, 1H, *J* = 7.5). Anal. Calcd. for $C_{16}H_{25}N_3O_3$, C 62.52, H 8.20, N 13.67. Found C 62.31, H 8.44, N 13.51.

*3.2.9. N-Isopentyl-2-(2′-oxo-3,4,5,6-tetrahydro-2H,2′H-[1,4′] bipyridinyl-1′-yl)acetamide (**1i**)*

Yield 29%. R_f = 0.54 ($CHCl_3$/MeOH 95:5). ^1H NMR (300 MHz, $CDCl_3$): δ 0.87 (d, 6H, *J* = 6.5 Hz), 1.33–1.40 (m, 2H), 1.51–1.63 (m, 7H), 3.16–3.23 (m, 2H), 3.30–3.33 (m, 4H), 4.41 (s, 2H), 5.72 (d, 1H, *J* = 2.9 Hz), 5.98 (dd, 1H, *J* = 7.6, 2.9 Hz), 7.16 (d, 1H, *J* = 7.6), 7.32 (bs, 1H). Anal. Calcd. for $C_{17}H_{27}N_3O_2$, C 66.85, H 8.91, N 13.76. Found C 66.87, H 8.84, N 13.88.

*3.3. General procedure for the synthesis of compounds **2a**–**c**, **2e**–**h**, and **2j***

The coupling between acids (**6**–**7**) and the suitable amines (1 equiv.) was carried out by employing HOBt (1.2 equiv.), EDCI (1.2 equiv.), DIPEA (2 equiv.) in dry CH_2Cl_2 at 0 °C. Then the mixture was stirred at room temperature for 12 h. The resulting mixture was washed with $KHSO_4$ 0.1 M, $NaHCO_3$ and brine. The crude product was purified by column chromatography ($CHCl_3$/MeOH 95:5).

*3.3.1. N-Benzyl-2-(2-oxopyridin-1(2H)-yl)acetamide (**2a**)*

Yield 86%. R_f = 0.52 ($CHCl_3$/MeOH 95:5). ^1H NMR (300 MHz, $CDCl_3$): δ 4.41 (d, 2H, *J* = 5.9 Hz), 4.58 (m, 2H), 6.24–6.29 (m, 1H), 6.59 (dd, 1H, *J* = 8.8, 1.2 Hz), 7.20–7.43 (m, 8H). Anal. Calcd. for $C_{14}H_{14}N_2O_2$, C 69.41, H 5.82, N 11.56. Found C 69.29, H 5.97, N 11.44.

*3.3.2. 2-(2-Oxopyridin-1(2H)-yl)-N-phenylacetamide (**2b**)*

Yield 77%. R_f = 0.41 ($CHCl_3$/MeOH 95:5). ^1H NMR (300 MHz, DMSO-d_6): δ 4.71 (s, 2H), 6.20–6.25 (m, 1H), 6.37 (d, 1H, *J* = 9.2), 7.0 3 (t, 1H, *J* = 7.5), 7.26–7.65 (m, 6H). Anal. Calcd. for $C_{13}H_{12}N_2O_2$, C 68.41, H 5.30, N 12.27. Found C 68.67, H 5.14, N 12.29.

*3.3.3. N-(4-Methoxyphenyl)-2-(2-oxopyridin-1(2H)-yl)acetamide (**2c**)*

Yield 79%. R_f = 0.45 ($CHCl_3$/MeOH 95:5). ^1H NMR (300 MHz, DMSO-d_6): δ 3.69 (s, 3H), 4.67 (s, 2H), 6.21 (m, 1H), 6.37 (m, 1H), 6.36 (d, 1H, *J* = 9.7 Hz), 6.86 (d, 2H, *J* = 8.8 Hz) 7.39–7.64 (m, 6H). Anal. Calcd. for $C_{14}H_{14}N_2O_3$, C 65.11, H 5.46, N 10.85. Found C 65.22, H 5.31, N 10.77.

*3.3.4. N-Adamant-1-yl-2-(2-oxo-2H-pyridin-1-yl)acetamide (**2e**)*

Yield 71%. R_f = 0.41 ($CHCl_3$/MeOH 95:5). ^1H NMR (300 MHz, $CHCl_3$): δ 1.63 (s, 6H), 1.88–2.02 (m, 10H), 4.43 (s, 2H), 6.21–6.26 (m, 1H), 6.61 (d, 1H, *J* = 9.7 Hz), 7.36–7.41 (m, 2H). Anal. Calcd. for $C_{17}H_{22}N_2O_2$, C 71.30, H 7.74, N 9.78. Found 71.43, H 7.48, N 9.83.

*3.3.5. N-Benzyl-2-(2-oxo-4-phenylamino-pyridin-1(2H)-yl) acetamide (**2f**)*

Yield 57%. R_f = 0.46 ($CHCl_3$/MeOH 95:5). ^1H NMR (300 MHz, DMSO-d_6): δ 4.27 (d, 2H, *J* = 6.2 Hz), 4.43 (s, 2H), 5.70 (d, 1H, *J* = 2.6 Hz) 5.92 (dd, 1H, *J* = 7.5, 2.6 Hz), 7.02–7.39 (m, 10H), 8.56 (t, 1H, *J* = 6.2 Hz). Anal. Calcd. for $C_{20}H_{19}N_3O_2$, C 72.05, H 5.74, N 12.60. Found C 72.35, H 5.49, N 12.99.

*3.3.6. 2-(2-Oxo-4-phenylamino-pyridin-1-(2H)-yl)-N-phenyl acetamide (**2g**)*

Yield 63%. R_f = 0.31 ($CHCl_3$/MeOH 95:5). ^1H NMR (300 MHz, DMSO): δ 4.55 (s, 2H), 5.90–5.93 (m, 1H), 6.15 (s, 1H), 7.09–7.72 (m, 11H), 8.55 (bs, 1H). Anal. Calcd. for $C_{19}H_{17}N_3O_2$, C 71.46, H 5.37, N 13.16. Found C 71.43, H 5.57, N 13.11.

*3.3.7. N-(4-Methoxyphenyl)-2-(2-oxo-4-phenylamino-pyridin-1-(2H)-yl)acetamide (**2h**)*

Yield 67%. R_f = 0.35 ($CHCl_3$/MeOH 95:5). ^1H NMR (300 MHz, DMSO-d_6): δ 3.70 (s, 3H), 4.52 (s, 2H), 5.80–5.91 (m, 1H), 6.17 (s,

1H), 6.45–7.32 (m, 10H), 8.57 (bs, 1H). Anal. Calcd. (%) for $C_{20}H_{19}N_3O_3$, C 68.75, H 5.48, N 12.03. Found C 68.69, H 5.88, N 12.01.

3.3.8. N-Adamant-1-yl-2-(2-oxo-4-phenylamino-2H-pyridin-1-yl) acetamide (**2j**)

Yield 61%. R_f = 0.22 ($CHCl_3$/MeOH 95:5). ^{1}H NMR (300 MHz, CD_3OH): δ 1.71 (s, 6H), 1.99–2.09 (m, 10H), 5.94 (d, 1H, J = 2.3), 6.11 (dd, 1H, J = 7.6, 2.3 Hz), 6.11 (dd, 1H, J = 7.6, 2.3 Hz), 8.60 (bs, 1H). Anal. Calcd. for $C_{23}H_{27}N_3O_2$, C 73.18, H 7.21, N 11.13. Found C 73.28, H 7.11, N 11.55.

3.4. General procedure for the synthesis of compounds **2d** and **2i**

For the synthesis of amides **2d** and **2i**, a suspension of acids **6** and **7** in dry CH_2Cl_2 was treated with N-methylmorpholine (1.1 equiv.) and isobutylchloroformate (1.1 equiv.) at 0 °C. After 30 min, a solution of 2-aminobenzophenone in dry CH_2Cl_2 was added to the refluxing mixture and the resulting solution was stirred at room temperature for 12 h. The organic layer was washed with brine:HCl 1 N (3:1). The crude product was purified by column chromatography ($CHCl_3$/MeOH 95:5).

3.4.1. N-(2-Benzoylphenyl)-2-(2-oxo-2H-pyridin-1-yl)acetamide (**2d**)

Yield 55%. R_f = 0.32 ($CHCl_3$/MeOH 95:5). ^{1}H NMR (300 MHz, DMSO-d_6): δ 5.12 (s, 2H), 6.19–6.24 (m, 1H), 6.38 (d, 1H, J = 8.3 Hz), 7.41–7.78 (m, 8H), 8.03–8.09 (m, 1H), 9.58–9.61 (m, 1H). Anal. Calcd. (%) for $C_{20}H_{16}N_2O_3$, C 72.28, H 4.85, N 8.43. Found C 72.48, H 4.56, N 8.74.

3.4.2. N-(2-Benzoylphenyl)-2-(2-oxo-4-phenylamino-2H-pyridin-1-yl)acetamide (**2i**)

Yield 53%. R_f = 0.58 ($CHCl_3$/MeOH 95:5). ^{1}H NMR (300 MHz, CD_3OH): δ 4.55 (s, 2H), 5.91–5.93 (m, 1H), 6.15 (dd, 1H, J = 7.5, 2.2 Hz), 7.09–7.72 (m, 14H), 8.12 (d, 1H, J = 7.9 Hz), 8.69 (bs, 1H). Anal. Calcd. (%) for $C_{26}H_{21}N_3O_3$, C 73.74, H 5.00, N 9.92. Found C 73.94, H 4.88, N 9.99.

3.5. Computational chemistry

Molecular modeling and graphics manipulations were performed using Maestro 9.2 (Schrödinger) [26] and UCSF-CHIMERA software packages [27], running on an E4 Computer Engineering E1080 workstation provided of an Intel Core i7-930 Quad-Core processor. GOLD 5.2 [28,29] was used for all docking calculations. Figures were generated using Pymol 1.0 [30].

3.5.1. Protein and ligands preparation

Coordinates for the chymotrypsin-like β5 subunit derived from the X-ray crystal structure of the yeast 20S proteasome determined at 2.8 Å resolution (PDB ID: 2F16) were employed for the automated docking studies [23]. The protein setup was carried out by Protein Preparation Wizard in Maestro. Hydrogen atoms were added to the protein consistent with the neutral physiologic pH. Arginine and lysine side chains were considered as cationic at the guanidine and ammonium groups, and the aspartic and glutamic residues were considered as anionic at the carboxylate groups. The crystal structure of 20S/bortezomib complex revealed one well-defined water molecule in proximity to D114O$^{\gamma}$, which coordinates a tight H-bonding network, interacting with β6-D114O$^{\gamma}$, β5-A49N and β5-A50N of the protein and with the C=O oxygen of bortezomib [23]. Moreover, one of the pyrazine nitrogens of bortezomib was found to interact *via* a direct H-bond with the protonated β6-D114. In fact, it has been observed that the pKa of pyrazine is approximately 1.0 and thus β6-D114 is most likely protonated. This is supported by the fact that in the X-ray structure the O–N distance is 2.9 Å, indicative of a strong H-bond. Accordingly, the intervening water molecule and the proper protonation state of D114 were included in the docking experiments. The protonation and flip states of the imidazole rings of the histidine residues were adjusted together with the side chain amides of glutamine and asparagine residues in an H-bonding network optimization process. Successively, the protein hydrogens only were minimized using the Impref module of Impact with the OPLS_2005 force field. The initial structures of **1b**, **1f** and **2h** were created, modified and energy-minimized with Schrödinger's Maestro [26].

3.5.2. Docking studies

Compounds **1b**, **1f** and **2h** were docked to the binding pocket of β5 subunit using GOLD, version 5.2 [28,29]. A radius of 20 Å from the β5 catalytic N-terminal threonine was used to direct site location. For each of the genetic algorithm runs, a maximum of 100,000 operations were performed on a population of 100 individuals with a selection pressure of 1.1. Operator weights for crossover, mutation, and migration were set to 95, 95, and 10, respectively, as recommended by the authors of the software. The distance for H-bonding was set to 2.5 Å, and the cutoff value for van der Waals calculation was set to 4 Å. The crystallographically determined water molecule near β6-D114 was specified in GOLD by switching state settings to 'toggle' and orientation mode to 'spin'. The Goldscore-CS docking protocol [31] was adopted in this study. In this protocol, the poses obtained with the original GoldScore function are rescored and reranked with the GOLD implementation of the ChemScore function [19,31–35]. To perform thorough and unbiased search of the conformation space, each docking run was allowed to produce 200 poses without the option of early termination, using standard default settings. The top solution obtained after re-ranking of the poses with ChemScore was selected to generate the proteasome/ligand complexes.

3.6. Pharmacology

3.6.1. In vitro 20S proteasome inhibition assays

Human 20S proteasome was obtained from Biomol GmbH, Hamburg, Germany. The three distinct proteolytic activities of the 20S proteasome were measured by monitoring the hydrolysis of the peptidyl 7-amino-4-methyl coumarin substrates (all obtained from Bachem) Suc-Leu-Leu-Val-Tyr-AMC, Boc-Leu-Arg-Arg-AMC, and Cbz-Leu-Leu-Glu-AMC for ChT-L, T-L and PGPH activity of the enzyme, respectively. Fluorescence of the product AMC of the substrates' hydrolyses was measured using an Infinite 200 PRO microplate reader (Tecan, Männedorf, Switzerland) at 30 °C with a 380 nm excitation filter and a 460 nm emission filter. The preliminary screening for the inhibition of the three proteolytic activities of the 20S proteasome was performed at 20 μM inhibitor concentrations using an equivalent amount of DMSO as a negative control. Compounds showing at least 40% inhibition at 20 μM were subjected to detailed assays. The dissociation constants K_i of the non covalent complex E·I were obtained from progress curves (10 min) at various concentrations of inhibitor by fitting the slopes of the progress curves to a 4 parameter IC_{50} equation, and correction to zero substrate concentration from $K_i = IC_{50}/(1 + [S]\ K_m^{-1})$. The K_m values were determined in separate experiments: ChT-L activity with Suc-Leu-Leu-Val-Tyr-AMC 13 μM, and PGPH activity with Cbz-Leu-Leu-Glu-AMC 53 μM.

3.6.2. Assaying the chymotryptic activity of the 20S proteasome

Human 20S proteasome was incubated at 30 °C at a final concentration of 0.004 mg mL^{-1} with test compound present at variable concentrations. The reaction buffer consisted of 50 mM Tris pH

7.5, 10 mM NaCl, 25 mM KCl, 1 mM $MgCl_2$, 0.03% SDS, and 5% DMSO. Product release from substrate hydrolysis (75 μM) was monitored continuously over a period of 10 min.

3.6.3. Assaying the tryptic activity of the 20S proteasome

Human 20S proteasome was incubated at 30 °C at a final concentration of 0.0025 mg mL^{-1} with test compound present at 20 μM. The reaction buffer consisted of 50 mM Tris buffer pH 7.4, 50 mM NaCl, 0.5 mM EDTA, 0.03% SDS, and 7.5% DMSO. Product release from substrate hydrolysis (85 μM) was monitored continuously over a period of 10 min.

3.6.4. Assaying the post glutamyl-peptide hydrolyzing activity of the 20S proteasome

Human 20S proteasome was incubated at 30 °C at a final concentration of 0.004 mg mL^{-1} with the test compound present at variable concentrations. The reaction buffer consisted of 50 mM Tris buffer pH 7.5 containing 25 mM KCl, 10 mM NaCl, 1 mM $MgCl_2$, 0.03% SDS, 5% DMSO. Product release from substrate hydrolysis (80 μM) was monitored continuously over a period of 10 min.

3.6.5. Assays for bovine pancreatic α-chymotrypsin inhibition

The enzyme (250 μg mL^{-1}) was incubated at 20 °C with test compound. The reaction buffer consisted of 50 mM Tris buffer pH 8.0 containing 100 mM NaCl and 5 mM EDTA and 7.5% DMSO. Product release from substrate hydrolysis (75 μM final concentration, Suc-Leu-Leu-Val-Tyr-AMC from Bachem) was determined over a period of 10 min.

3.6.6. Assays for cathepsin B inhibition

Assays with cathepsins B were performed as described previously [36]. Cbz-Phe-Arg-AMC was used as substrate (80 μM). The K_m value used to calculate K_i values from IC_{50} values was 150 μM.

Acknowledgments

This work was financially supported by the Ministero dell'Istruzione, dell'Università e della Ricerca Scientifica e Tecnologica [MIUR-PRIN2010-2011, grant N° 2010W7YRLZ_003 (A.L.) and 2010W7YRLZ_004 (S.G.)]. We would like to thank the Deutscher Akademischer Austausch Dienst (DAAD) (Vigoni project 2011/12) for partial support of this work. T.S. thanks the Deutsche Forschungsgemeinschaft (DFG) for financial support. R.E. acknowledges the support of her postdoctoral fellowship from "Dote Ricerca": FSE, Regione Lombardia.

References

[1] M. Unno, T. Mizushima, Y. Morimoto, Y. Tomisugi, K. Tanaka, N. Yasuoka, T. Tsukihara, The structure of the mammalian 20S proteasome at 2.75 Å resolution, Structure 10 (2002) 609–618.
[2] M. Groll, L. Ditzel, J. Lowe, M. Bochtler, H.D. Bartunik, R. Huber, Structure of 20S proteasome from yeast at 2.4 Å resolution, Nature 386 (1997) 463–471.
[3] P.M. Kloetzel, Antigen processing by the proteasome, Nat. Rev. Mol. Cell Biol. 2 (2001) 179–187.
[4] A. Sacco, M. Aujay, B. Morgan, A.K. Azab, P. Mais, Y. Liu, Y. Zhang, F. Azab, H.T. Ngo, G.C. Issa, P. Quang, A.M. Roccaro, I.M. Ghobria, Chymotrypsin-like activity of the proteasome leads to antitumor carfilzomib-dependent selective inhibition of the activity in Waldenstrom's macroglobulinemia, Clin. Cancer Res. 17 (2011) 1753–1764.
[5] (a) S. Meiners, A. Ludwig, V. Stangl, K. Stangl, Proteasome inhibitors: poisons and remedies, Med. Res. Rev. 28 (2008) 309–327;
b) E.M. Huber, M. Groll, Inhibitors for the immuno- and constitutive proteasome: current and future trends in drug development, Angew. Chem. Int. Ed. 51 (2012) 8708–8720.
[6] J. Wang, M.A. Maldonado, The ubiquitin–proteasome system and its role in inflammatory and autoimmune diseases, Cell. Mol. Immunol. 3 (2006) 255–261.
[7] B. Skaug, X. Jiang, Z.J. Chen, The role of ubiquitin in NFkappaB regulatory pathways, Annu. Rev. Biochem. 78 (2009) 769–796.
[8] a) G. Bonuccelli, F. Sotgia, F. Capozza, E. Gazzerro, C. Minetti, M.P. Lisanti, Localized treatment with a novel FDA-approved proteasome inhibitor blocks the degradation of dystrophin and dystrophin-associated proteins in mdx mice, Cell Cycle 6 (2007) 1242–1248;
b) B.A. Azakir, S. Di Fulvio, J. Kinter, M. Sinnreich, Proteasomal inhibition restores biological function of mis-sense mutated dysferlin in patient-derived muscle cells, J. Biol. Chem. 287 (2012) 10344–10354.
[9] R.T. Jagoe, A.L. Goldberg, What do we really know about the ubiquitin–proteasome pathway in muscle atrophy? Curr. Opin. Clin. Nutr. Metab. Care 4 (2001) 183–190.
[10] a) C. Lindenthal, N. Weich, Y.S. Chia, V. Heussler, M.Q. Klinkert, The proteasome inhibitor MLN-273 blocks exoerythrocytic and erythrocytic development of Plasmodium parasites, Parasitology 131 (Part 1) (2005) 37–44;
b) H. Li, E.L. Ponder, M. Verdoes, K.H. Asbjornsdottir, E. Deu, L.E. Edgington, J.T. Lee, C.J. Kirk, S.D. Demo, K.C. Williamson, M. Bogyo, Validation of the proteasome as a therapeutic target in Plasmodium using an epoxyketone inhibitor with parasite-specific toxicity, Chem. Biol. 19 (2012) 1535–1545.
[11] a) Z. Li, C.B. Zou, Y. Yao, M.A. Hoyt, S. McDonough, Z.B. Mackey, P. Coffino, C.C. Wang, An easily dissociated 26S proteasome catalyzes an essential ubiquitin-mediated protein degradation pathway in *Trypanosoma brucei*, J. Biol. Chem. 277 (2002) 15486–15498;
b) D. Steverding, The proteasome as a potential target for chemotherapy of African trypanosomiasis, Drug Dev. Res. 68 (2007) 205–212;
c) D. Steverding, X. Wang, B.C. Potts, M.A. Palladino, Trypanocidal activity of beta-lactone-gamma-lactam proteasome inhibitors, Planta Med. 78 (2012) 131–134.
[12] G. Lin, D. Li, L.P. de Carvalho, H. Deng, H. Tao, G. Vogt, K. Wu, J. Schneider, T. Chidawanyika, J.D. Warren, H. Li, C. Nathan, Inhibitors selective for mycobacterial versus human proteasomes, Nature 461 (2009) 621–626.
[13] P. Beck, C. Dubiella, M. Groll, Covalent and non-covalent reversible proteasome inhibition, Biol. Chem. 393 (2012) 1101–1120.
[14] S. Arastu-Kapur, J.L. Anderl, M. Kraus, F. Parlati, K.D. Shenk, S.J. Lee, T. Muchamuel, M.K. Bennett, C. Driessen, A.J. Ball, et al., Nonproteasomal targets of the proteasome inhibitors bortezomib and carfilzomib: a link to clinical adverse events, Clin. Cancer Res. 17 (2011) 2734–2743.
[15] (a) R. Ettari, L. Tamborini, I.C. Angelo, N. Micale, A. Pinto, C. De Micheli, P. Conti, Inhibition of rhodesain as a novel therapeutic modality for human African trypanosomiasis, J. Med. Chem. 56 (2013) 5637–5658;
(b) R. Ettari, M. Zappalà, N. Micale, G. Grazioso, S. Giofrè, T. Schirmeister, S. Grasso, Peptidomimetics containing a vinyl ketone warhead as falcipain-2 inhibitors, Eur. J. Med. Chem. 46 (2011) 2058–2065;
(c) F. Bova, R. Ettari, N. Micale, C. Carnovale, T. Schirmeister, C. Gelhaus, M. Leippe, S. Grasso, M. Zappalà, Constrained peptidomimetics as antiplasmodial falcipain-2 inhibitors, Bioorg. Med. Chem. 18 (2010) 4928–4938;
(d) N. Micale, R. Ettari, T. Schirmeister, A. Evers, C. Gelhaus, M. Leippe, M. Zappalà, S. Grasso, Novel 2*H*-isoquinolin-3-ones as antiplasmodial falcipain-2 inhibitors, Bioorg. Med. Chem. 17 (2009) 6505–6511;
(e) R. Ettari, M. Zappalà, N. Micale, T. Schirmeister, C. Gelhaus, M. Leippe, A. Evers, S. Grasso, Synthesis of novel peptidomimetics as inhibitors of protozoan cysteine proteases falcipain-2 and rhodesain, Eur. J. Med. Chem. 45 (2010) 3228–3233.
[16] (a) M. Groll, N. Gallastegui, X. Maréchal, V. Le Ravalec, N. Basse, N. Richy, E. Genin, R. Huber, L. Moroder, J. Vidal, M. Reboud-Ravaux, 20S proteasome inhibition: designing noncovalent linear peptide mimics of the natural product TMC-95A, ChemMedChem 5 (2010) 1701–1705;
(b) E. Genin, M. Reboud-Ravaux, J. Vidal, Proteasome inhibitors: recent advances and new perspectives in medicinal chemistry, Curr. Top. Med. Chem. 10 (2010) 232–256.
[17] J. Kaffy, G. Bernadat, S. Ongeri, Non-covalent proteasome inhibitors, Curr. Pharm. Des. 19 (2013) 4115–4130.
[18] R. Ettari, C. Bonaccorso, N. Micale, C. Heindl, T. Schirmeister, M.L. Calabrò, S. Grasso, M. Zappalà, Development of novel peptidomimetics containing a vinyl sulfone moiety as proteasome inhibitors, ChemMedChem 6 (2011) 1228–1237.
[19] N. Micale, R. Ettari, A. Lavecchia, C. Di Giovanni, K. Scarbaci, V. Troiano, S. Grasso, E. Novellino, T. Schirmeister, M. Zappalà, Development of peptidomimetic boronates as proteasome inhibitors, Eur. J. Med. Chem. 64 (2013) 23–34.
[20] (a) R.T. Lum, M.G. Nelson, A. Joly, A.G. Horsma, G. Lee, S.M. Meyer, M.M. Wick, S.R. Schow, Selective inhibition of the chymotrypsin-like activity of the 20S proteasome by 5-methoxy-1-indanone dipeptide benzamides, Bioorg. Med. Chem. Lett. 8 (1998) 209–214;
(b) C. Garcìa-Echeverrìa, P. Imbach, D. France, P. Fürst, M. Lang, M. Noorani, D. Scholz, J. Zimmermann, P. Furet, A new structural class of selective and non-covalent inhibitors of the chymotrypsin-like activity of the 20S proteasome, Bioorg. Med. Chem. Lett. 11 (2001) 1317–1319.
[21] H.R. Snyder, J.A. Kuck, J.R. Johnson, Organoboron compounds, and the study of reaction mechanisms. Primary aliphatic boronic acids, J. Am. Chem. Soc. 60 (1938) 105–111.
[22] J.R. Johnson, M.G. Van Campen Jr., O. Grummit, Organoboron compounds. II. The reducing action of some organoboronic acids, J. Am. Chem. Soc. 60 (1938) 111–115.
[23] M. Groll, C.R. Berkers, H.L. Ploegh, H. Ovaa, Crystal structure of the boronic acid-based proteasome inhibitor bortezomib in complex with the yeast 20S proteasome, Structure 14 (2006) 451–456.

[24] M. Groll, R. Huber, B.C. Potts, Crystal structures of salinosporamide A (NPI-0052) and B (NPI-0047) in complex with the 20S proteasome reveal important consequences of β-lactam ring opening and a mechanism for irreversible binding, J. Am. Chem. Soc. 128 (2006) 5136–5141.
[25] (a) E.J. Corey, W.D. Li, Total synthesis and biological activity of lactacystin, omuralide and analogs, Chem. Pharm. Bull. 47 (1999) 1–10;
b) M. Nett, T.A. Gulder, A.J. Kale, C.C. Hughes, B.S. Moore, Function-oriented biosynthesis of beta-lactone proteasome inhibitors in *Salinispora tropica*, J. Med. Chem. 52 (2009) 6163–6167.
[26] Maestro, Version 9.2, Schrödinger, LLC, New York, NY, 2011.
[27] C.C. Huang, G.S. Couch, E.F. Pettersen, T.E. Ferrin, Chimera: an extensible molecular modelling application constructed using standard components, Pac. Symp. Biocomput. 1 (1996) 724. http://www.cgl.ucsf.edu/chimera.
[28] G. Jones, P. Willett, R.C. Glen, A.R. Leach, R. Taylor, Development and validation of a genetic algorithm for flexible docking, J. Mol. Biol. 267 (1997) 727–748.
[29] GOLD, Version 5.2, The Cambridge Crystallographic Data Centre, Cambridge, U.K., 2012.
[30] W.L. DeLano, The PyMOL Molecular Graphics System, DeLano Scientific LLC, San Carlos, CA, USA, http://www.pymol.org/.
[31] M.L. Verdonk, J.C. Cole, M.J. Hartshorn, C.W. Murray, R.D. Taylor, Improved protein-ligand docking using GOLD, Proteins Struct. Funct. Genet. 52 (2003) 609–623.
[32] G. Fracchiolla, A. Laghezza, L. Piemontese, P. Tortorella, F. Mazza, R. Montanari, G. Pochetti, A. Lavecchia, E. Novellino, S. Pierno, D. Conte Camerino, F. Loiodice, New 2-aryloxy-3-phenyl-propanoic acids as PPAR α/γ dual agonists with improved potency and reduced adverse effects on skeletal muscle function, J. Med. Chem. 52 (2009) 6382–6393.
[33] C. La Motta, S. Sartini, L. Mugnaini, S. Salerno, F. Simorini, S. Taliani, A.M. Marini, F. Da Settimo, A. Lavecchia, E. Novellino, L. Antonioli, M. Fornai, C. Blandizzi, M. Del Tacca, Exploiting the pyrazolo[3,4-*d*]pyrimidin-4-one ring system as a useful template to obtain potent adenosine deaminase inhibitors, J. Med. Chem. 52 (2009) 1681–1692.
[34] L. Porcelli, F. Gilardi, A. Laghezza, L. Piemontese, N. Mitro, A. Azzariti, F. Altieri, L. Cervoni, G. Fracchiolla, M. Giudici, U. Guerrini, A. Lavecchia, R. Montanari, C. Di Giovanni, A. Paradiso, G. Pochetti, G.M. Simone, P. Tortorella, M. Crestani, F. Loiodice, Synthesis, characterization and biological evaluation of ureidofibrate-like derivatives endowed with peroxisome proliferator-activated receptor activity, J. Med. Chem. 55 (2012) 37–54.
[35] M.G. Perrone, P. Vitale, P. Malerba, A. Altomare, A. Lavecchia, C. Di Giovanni, E. Novellino, A. Scilimati, Core ring nature in diarylheterocycle COX-1 inhibitors, ChemMedChem 7 (2012) 629–641.
[36] (a) R. Vicik, M. Busemann, C. Gelhaus, N. Stiefl, J. Scheiber, W. Schmitz, F. Schulz, M. Mladenovic, B. Engels, M. Leippe, K. Baumann, T. Schirmeister, Aziridide-based inhibitors of cathepsin L: synthesis, inhibition activity, and docking studies, ChemMedChem 1 (2006) 1126–1141;
(b) R. Ettari, E. Nizi, M.E. Di Francesco, M.A. Dude, G. Pradel, R. Vicik, T. Schirmeister, N. Micale, S. Grasso, M. Zappalà, Development of peptidomimetics with a vinyl sulfone warhead as irreversible falcipain-2 inhibitors, J. Med. Chem. 51 (2008) 988–996.